Structures in the excitation functions of high lying inelastic channels of the $^{16}O+^{16}O$ system in the region $E_{c.m.}=26$ to 47 MeV

B. J. Greenhalgh, G. K. Dillon, B. R. Fulton, D. L. Watson, and R. L. Cowin
Department of Physics, University of York, Heslington, York Y010 5DD, United Kingdom

M. Freer and S. M. Singer
School of Physics and Astronomy, University of Birmingham, Edgbaston, Birmingham B15 2TT, United Kingdom

S. P. G. Chappell, C. A. Bremner, and W. D. M. Rae
Nuclear and Astrophysics Laboratory, University of Oxford, Keble Road, Oxford OX1 3RH, United Kingdom

D. C. Weisser
Department of Nuclear Physics, Australian National University, Canberra ACT 0200, Australia
(Received 10 March 2003; published 24 May 2004)

An excitation function measurement has been performed over the laboratory range 52–94 MeV investigating resonance phenomena in the single excitation ^{16}O ($^{16}O, ^{16}O^{*} \rightarrow ^{12}C_{g.s.}+\alpha)^{16}O_{g.s.}$ breakup reaction. A number of enhancements are observed in these excitation functions for excitation to the 4_1^+, 10.35 MeV and 4_2^+, 11.09 MeV excited states in ^{16}O. The overlap between these and previously measured enhancements is discussed. Excitation functions for the 2_2^+, 9.84 MeV and 2_3^+, 11.52 MeV excited states are also presented.

DOI: 10.1103/PhysRevC.69.054316 PACS number(s): 25.60.−t, 27.30.+t, 27.20.+n, 21.60.Gx

I. INTRODUCTION

The energy dependence of the cross sections of heavy-ion reactions has been a topic of considerable interest for over three decades [1]. The observation of resonances for elastic and inelastic reactions has provided substantial evidence for rotational bands of excited states in nuclei which may have clusterlike properties [2,3]. In particular the $^{12}C+^{12}C$ system has revealed a wide range of resonances, from narrow resonances at energies near the Coulomb barrier [1,4] to wider structures in inelastic scattering data [5,6]. Such resonance phenomena may be related to underlying cluster structure in these systems [7]. This paper is concerned with resonantlike structures observed in the $^{16}O+^{16}O$ system.

The data available on resonance phenomena in the $^{16}O+^{16}O$ system up to about 1986 have been summarized by Cindro [8]. As is the case with the more extensively studied $^{12}C+^{12}C$ system [3] the $^{16}O+^{16}O$ resonances indicate rotational characteristics. The moment of inertia associated with this rotation was found to be ~47 keV, in good agreement with the value of ~43 keV calculated for two ^{16}O nuclei in a dimolecular configuration [8].

Subsequent investigations of excitation functions for various $^{16}O+^{16}O$ reactions have mainly been concerned with inelastic channels, in particular the single and mutual excitation of $^{16}O^{*}$ to the 0_2^+, 6.05 MeV and 3_1^-, 6.13 MeV excited states. Pronounced correlated gross structure resonances have been observed in the excitation functions for the single and mutual excitation of ^{16}O to the 0_2^+, 6.05 MeV excited state [9–11] up to center-of-mass energies of 40 MeV. Similar studies investigating the excitation functions for the single and mutual excitation of ^{16}O to the 3_1^-, 6.13 MeV excited state have shown correlated resonances in both channels [12,13] up to $E_{c.m.}=40$ MeV.

The 0_2^+, 6.05 MeV excited state in ^{16}O has been shown to be largely $4p$-$4h$ in nature and is well established [14] as having a $^{12}C_{g.s.}-\alpha$ structure. It is recognized as being the first member of a $K^{\pi}=0^+$ rotational band with the other band members being suggested to be the 2_1^+, 6.91 MeV, 4_1^+, 10.35 MeV, and 6_2^+, 16.28 MeV excited states.

The 3_1^-, 6.13 MeV excited state is proposed to be the 3^- member of a tetrahedral rotational band in ^{16}O. This proposed band has an intrinsic spin sequence 0^+, 3^-, 4^+ with the corresponding energies proportional to $J(J+1)$ [15]. The 4^+ member is predicted at 10.2 MeV. However, the only 4^+ excited state in ^{16}O in this excitation region is the 4_1^+ at 10.35 MeV which has been assigned to the $K^{\pi}=0^+$ $4p$-$4h$ rotational band [16]. This assignment is justified by the fast $E2$ decay to the 2_1^+ member of the same band at 6.91 MeV [17] which in turn has a fast $E2$ decay to the 0_2^+, 6.05 MeV state which is believed to be the bandhead of this band [17]. The calculations of Buck *et al.* [18] predicted the energies, decay widths, and $E2$ transition values for many levels in ^{16}O. Based on these calculations the 4_1^+, 10.35 MeV state was proposed to have a structure of $^{12}C_{g.s.}+\alpha$, which fits in with the $4p$-$4h$ nature of the $K^{\pi}=0^+$ band. The 4_2^+ excited state at 11.09 MeV in ^{16}O has been proposed to be the 4^+ member of the tetrahedral band as an alternative candidate to the 4_1^+, 10.35 MeV state [19,20].

In this paper we report an extension of studies of $^{16}O+^{16}O$ scattering to higher lying inelastic states, in particular the next highest spin states 4_1^+, 10.35 MeV and 4_2^+, 11.09 MeV. To perform such studies through conventional two-body scattering measurements would be quite complex as both 4^+ states lie in a continuum of known states, around 10–11 MeV, with widths varying from a few keV to 2.5 MeV. It is reasonable to assume that resolving both 4^+ states by means of an inelastic scattering measurement

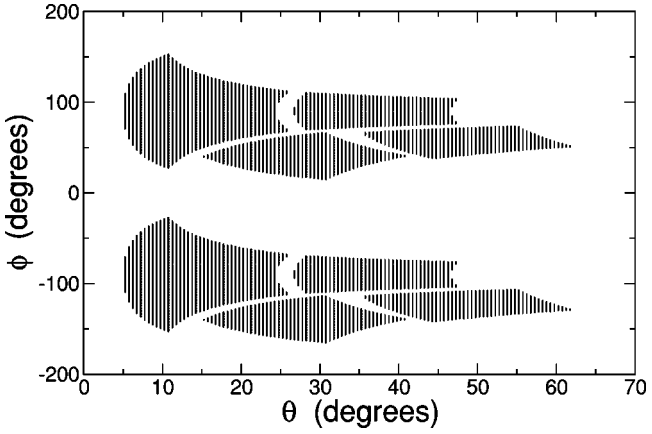

FIG. 1. Angular coverage of the detectors used in the measurement.

would be difficult. However, as both these states are above the α-particle decay threshold, an alternative approach would be the measurement and subsequent reconstruction of the decay fragments, $^{12}C+\alpha$. This technique has been implemented before in studies of the $^{12}C+^{12}C$ system [21] where states in ^{12}C above the α-particle decay threshold have been successfully reconstructed and resolved. This paper reports on a measurement of the excitation functions for single excitation to the 4_1^+, 10.35 MeV and 4_2^+, 11.09 MeV states in ^{16}O via the $^{16}O+^{16}O$ reaction, using such breakup measurement techniques.

II. EXPERIMENTAL DETAILS

The measurement was performed at the Australian National University (ANU) 14-UD accelerator using the new Charissa strip detector array located in the MEGHA scattering chamber [22]. Eight 500 μm thick, 50×50 mm^2 Si strip detectors were installed and covered an angular range of $\theta_{lab}=5°$ to 65° and an azimuthal angular range $\Delta\phi\approx120°$ each side of the beam axis. This provided a wide coverage for the multiple detection of breakup fragments. Figure 1 illustrates the laboratory angles covered by the detectors. Each strip detector consisted of 16 position sensitive strips, 3 mm wide, which were independently instrumented. Signals taken from both ends of a strip were used to reconstruct the total energy and the emission angle of the particle detected by that strip. Details of the operation of these detectors can be found elsewhere [23]. Calibration, both energy and position, was achieved by the elastic scattering of ^{16}O ions with a flash gold target (^{197}Au 5 μg cm^{-2} backed with 10 μg cm^{-2} of ^{12}C).

An excitation function over the laboratory range 52–94 MeV in steps of 2–4 MeV was performed using a beam of ^{16}O ions ($\sim$10 enA) accelerated onto a target of LiO (10 μg cm^{-2}) on a ^{12}C backing (10 μg cm^{-2}). The target was made as thin as possible to reduce energy loss.

III. DATA ANALYSIS

The experimental trigger requirement was a total strip multiplicity of greater than or equal to 3 particle hits. In this

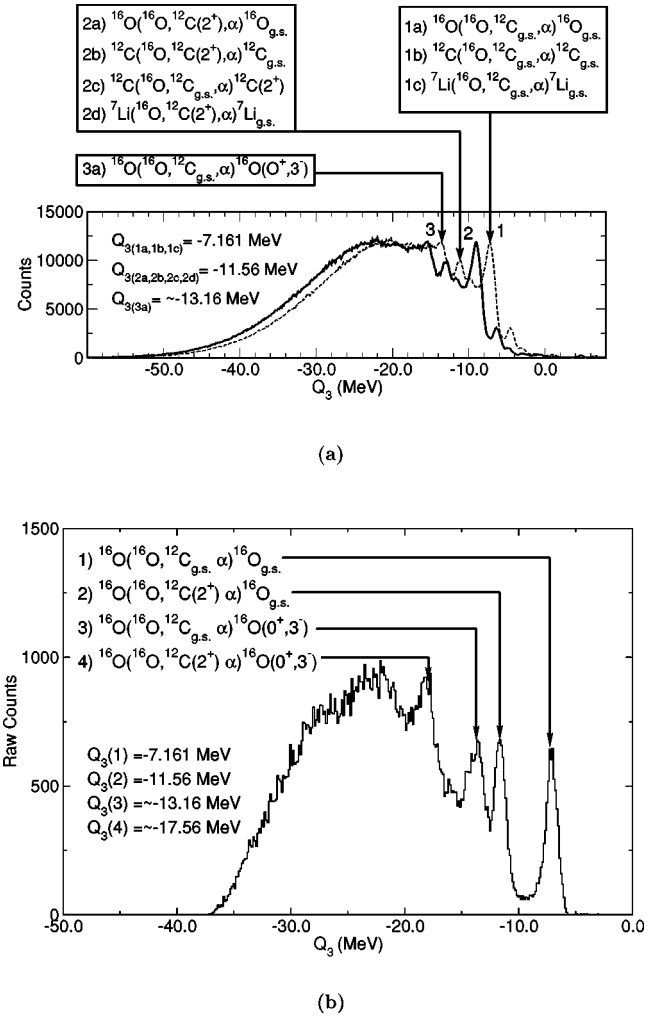

FIG. 2. Three-body Q values, Q_3, for $E_{lab}=73$ MeV of (a) raw multiplicity 3 data for a selection of reactions with all three target components and (b) data after the application of the various momentum and kinematic gates (described in the text). The dashed line represents the Q value with a $\sim$1.8 MeV offset applied.

way the measurement was then sensitive to the primary reaction of interest, $^{16}O(^{16}O,^{16}O^*\rightarrow{}^{12}C_{g.s.}+\alpha)^{16}O_{g.s.}$. No explicit particle identification was used during the measurement but an iterative technique based on final state mass assumption and comparing the total momenta in the x, y, and z (beam) directions with simulated Monte Carlo data allowed the final states to be correctly identified. This technique is similar to previously used methods of final state state selection [21].

Figure 2 shows the effect this iterative momentum gating procedure has on the total Q-value spectrum for all multiplicity 3 data determined from the summed measured energies of the final state particles. The three labeled peaks, 1, 2, and 3, in Fig. 2(a) represent a series of reactions with the same Q value prior to complete final state mass assignment. The substantially lower background level in Fig. 2(b) indicates that removal of the majority of ^{7}Li and ^{12}C recoil events has been successful. The offset of 1.8 MeV of the peaks in Fig. 2(a) is associated with errors in the calibration process at low energies due to the calibration with an ^{16}O

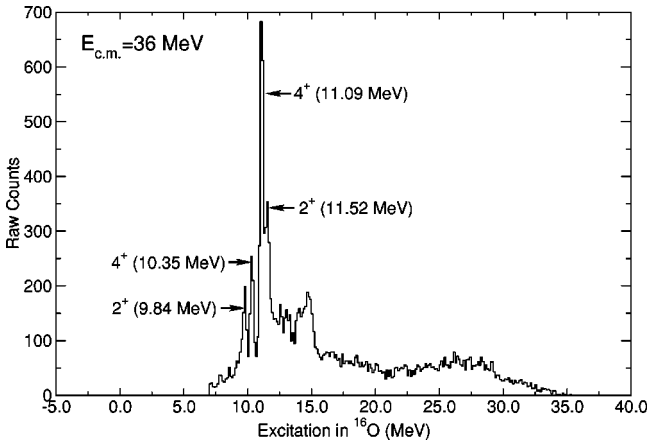

FIG. 3. Excited states associated with the reconstructed $^{16}O^{*}$ nucleus for $E_{\mathrm{c.m.}}=36$ MeV.

beam and the reaction process involved the detection of α particles. An additional offset was applied to correct for this. It can be seen from Fig. 2(b) that the reactions of interest are well isolated after the identification technique has been implemented. The background that is seen at negative Q values is attributed to reactions with a fourfold or greater final state where one or more of the final state nuclei has not been detected.

A software gate was then applied to the Q value spectrum in Fig. 2(b) in order to analyze the relevant reaction.

IV. RESULTS

The reaction $^{16}\mathrm{O}(^{16}\mathrm{O},^{16}\mathrm{O}^{*}\rightarrow{}^{12}\mathrm{C}_{\mathrm{g.s.}}+\alpha)^{16}\mathrm{O}_{\mathrm{g.s.}}$ was selected and the relative energy of the $^{12}\mathrm{C}_{\mathrm{g.s.}}$ and the α nucleus was then calculated [21]. This was then used to determine the excitation energy in the reconstructed $^{16}O^{*}$ parent nucleus. Figure 3 shows an excitation spectrum of $^{16}O^{*}$ for a center-of-mass energy of 36 MeV. Of particular interest in Fig. 3 are the excited states at 10.35 and 11.09 MeV as has already been discussed. Experimental yields for each of the states were then calculated for each beam energy used. The yields were determined by integrating the peaks in the excitation spectrum, which were fitted with a Gaussian distribution including a polynomial background term. The yields were then normalized for beam exposure at each of the different beam energies. The normalized experimental yields, proceeding from the 2_2^+, 9.84 MeV, 4_1^+, 10.35 MeV, 4_2^+, 11.09 MeV, and 2_3^+, 11.52 MeV excited states in ^{16}O are shown in Fig. 4. The relative detection efficiencies for each excitation energy determined from a Monte Carlo simulation incorporating the same angular cuts, energy thresholds, and resolutions as in the experimental data are also shown in Fig. 4. The profiles shown assume an exponential falloff for the primary scattering and an isotropic breakup of the excited states in ^{16}O in the center-of-mass frame and are seen to be smoothly varying with the center-of-mass energy.

In addition, an angular correlation investigation enabled a dominant partial wave (L, orbital angular momentum component) value to be associated with some of the enhance-

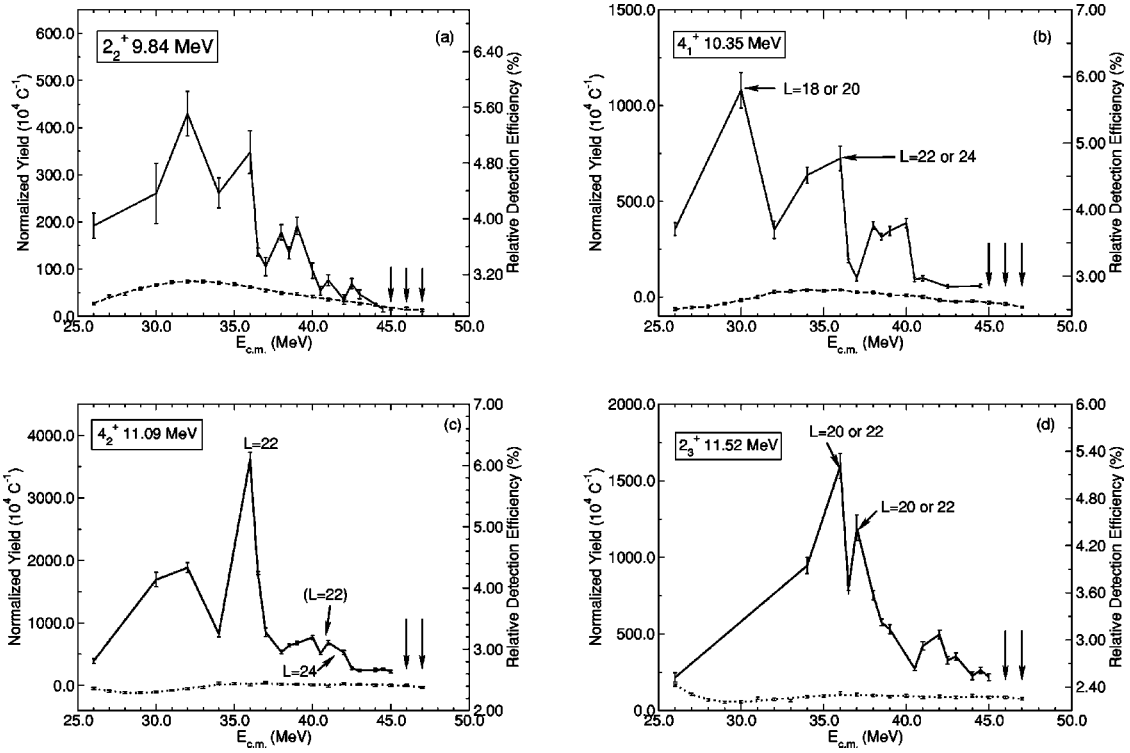

FIG. 4. Excitation functions for the $^{16}\mathrm{O}(^{16}\mathrm{O},^{16}\mathrm{O}^{*}\rightarrow{}^{12}\mathrm{C}_{\mathrm{g.s.}}+\alpha)^{16}\mathrm{O}_{\mathrm{g.s.}}$ breakup reaction proceeding from the (a) 2_2^+, 9.84 MeV (b) 4_1^+, 10.35 MeV (c) 4_2^+, 11.09 MeV, and (d) 2_3^+, 11.52 MeV excited states in $^{16}O^{*}$. The data are normalized to beam exposure only. The dashed line shows the relative detection efficiency profile determined form a Monte Carlo simulation. The vertical arrows indicate upper limits for the beam normalized yield where the particular channel could not be resolved from the background.

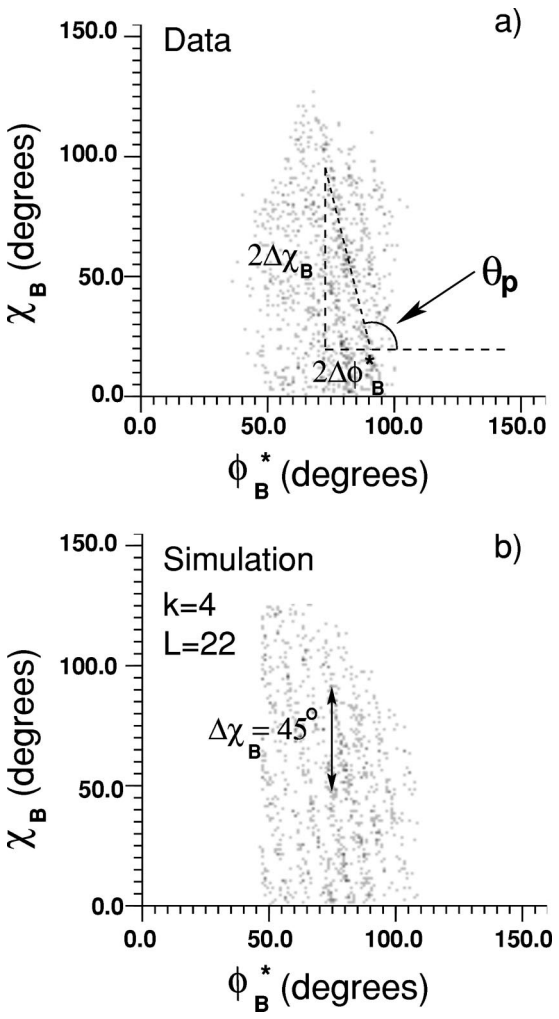

FIG. 5. Angular correlation for the reaction $^{16}O(^{16}O,^{16}O^* \rightarrow ^{12}C_{g.s.}+\alpha)^{16}O_{g.s.}$ for decay from the 4^+_2, 11.09 MeV excited state in ^{16}O at $E_{c.m.}=36$ MeV. (a) Experimental data (b) simulation data assuming $k=4$ (spin of the state) and $L=22$ (orbital angular momentum component).

ments observed in Fig. 4. The details of this angular correlation analysis are not described here but can be found elsewhere [24,25] and are similar to those used by Chappell *et al.* [26]. Briefly, after isolation of a specific decay had been achieved, a two-dimensional plot of the angles ϕ^* against χ^* (defined formally in the Basel coordinate system in Ref. [25]) was made. The angles ϕ^* and χ^* are the azimuthal components of θ^* and ψ^*, where θ^* represents the primary scattering angle in the center-of-mass frame and ψ^* characterizes the breakup by defining the orientation of the relative velocity vector between the decay fragments. This was then compared to a simulated angular correlation plot, assuming a semiclassical angular correlation function [25], where the simulated data are subject to the same cuts as the real data. An example of these two plots is given in Fig. 5 for the 4^+_2, 11.09 MeV excited state in ^{16}O. By projecting the real and simulated data onto the ϕ^* axis at an angle θ_p, which defines the optimum projection angle needed to maximize the peak to valley ratio of the ridge structure observed, the value of L can be varied in the simulations so that the periodicity of the simulated data matched the experimental data. The L value was assigned to the enhancement when the best match was achieved. The one-dimensional projections of the experimental and simulated angular correlations used to determine the L value of the enhancements observed in this work are shown in Figs. 6–8. Figures 6–8 show the projections for decay, for a selection of possible L values, from the 4^+_1, 10.35, 4^+_2, 11.09, and 2^+_3, 11.52 MeV states, respectively. The optimum projection angle θ_p and the center-of-mass energy are given in each figure. The assigned orbital angular momentum values L are shown in Fig. 4.

V. DISCUSSION

The excitation functions shown in Fig. 4 display a number of enhancements at various center-of-mass energies, some of which have a dominant partial wave associated with them. If we assume stretched coupling, then the total angular momen-

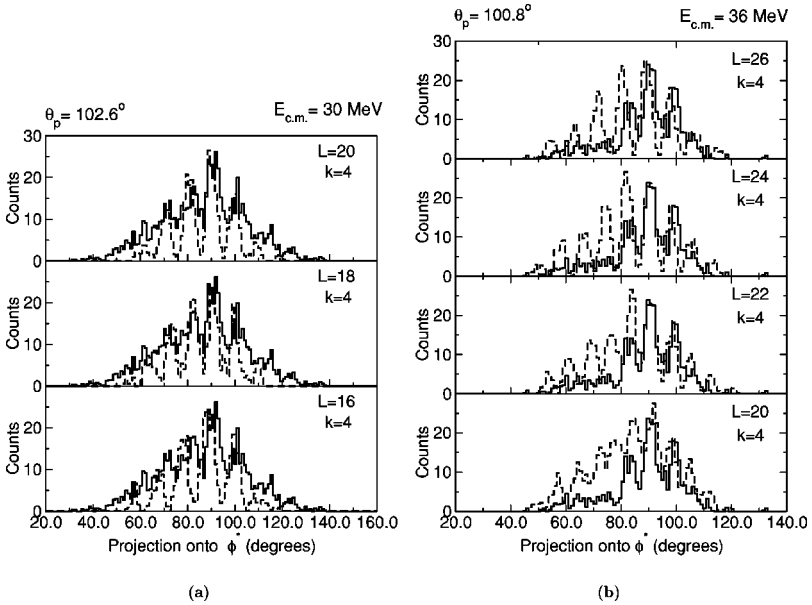

FIG. 6. One-dimensional projection of the measured angular correlation structure (solid line) on to a single axis (ϕ^*) for the reaction $^{16}O(^{16}O,^{16}O^*[4^+_1, 10.35\ \text{MeV}] \rightarrow ^{12}C_{g.s.}+\alpha)$ $^{16}O_{g.s.}$, compared with simulated angular correlation projections (dotted line) on to the same axis. The k and L values chosen for the simulation are shown on each plot. (a) The $E_{c.m.}=30$ MeV enhancement, (b) the $E_{c.m.}=36$ MeV enhancement.

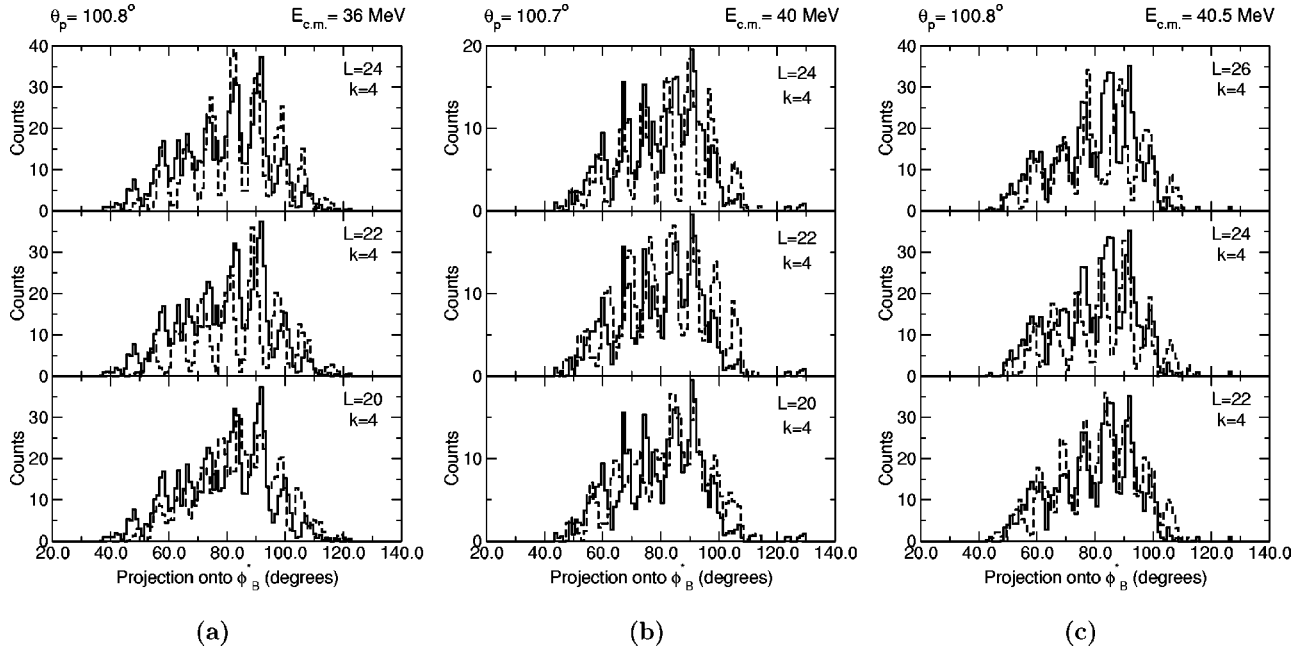

FIG. 7. One-dimensional projection of the measured angular correlation structure (solid line) on to a single axis (ϕ^*) for the reaction $^{16}O(^{16}O,^{16}O^*[4_2^+, 11.09\ \text{MeV}] \rightarrow {}^{12}C_{g.s.}+\alpha)^{16}O_{g.s.}$, compared with simulated angular correlation projections (dotted line) on to the same axis. The k and L values chosen for the simulation are shown on each plot. (a) The $E_{c.m.}=36$ MeV enhancement, (b) the $E_{c.m.}=40$ MeV enhancement, and (c) the $E_{c.m.}=40.5$ MeV enhancement.

tum or spin J of the enhancement is equal to $L+k$, where k is the intrinsic angular momentum projection, or spin of the excited state, and L is the previously discussed orbital angular momentum component.

A. The 4_1^+, 10.35 MeV and 4_2^+, 11.09 MeV excitation functions

1. 4_1^+, 10.35 MeV excitation function

All three enhancements observed in this excitation function, at $E_{c.m.} \simeq 30$ MeV, 36 MeV, and 39 MeV, seem to overlap with enhancements observed in the excitation functions for other exit channels associated with the $^{16}O+{}^{16}O$ system. The peak observed at $E_{c.m.} \simeq 30$ MeV has a similar center-of-mass energy to the enhancement observed in the excitation function for single excitation to the 3_1^-, 6.13 MeV state [13]. Pate *et al.* assigned this observed enhancement a spin of $J=20$ or 22. We have been able to assign a spin of $J=22$ or 24 to the peak observed in this investigation and therefore there appears to be some agreement. The structure observed at $E_{c.m.} \simeq 36$ MeV also appears to overlap with that observed in the same measurement performed by Pate *et al.* The assigned spin of $J=26$ or 28 is in good agreement with

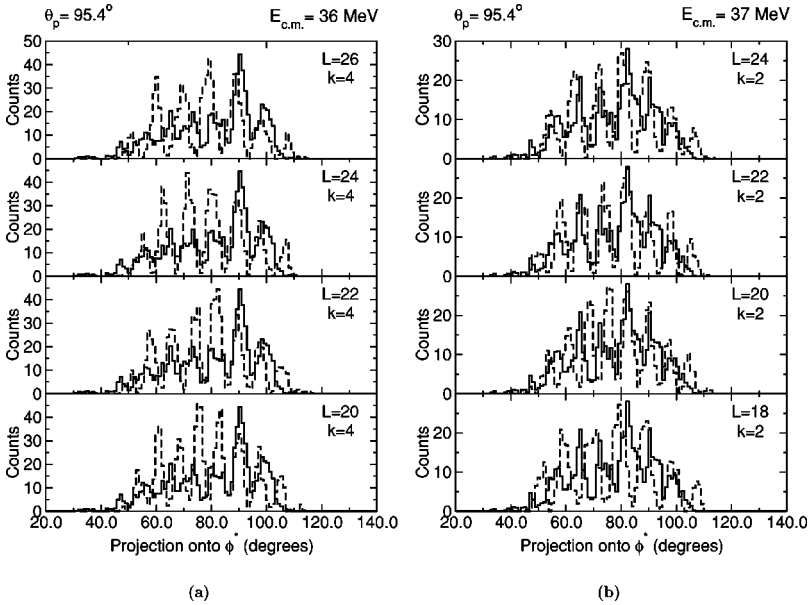

FIG. 8. One-dimensional projection of the measured angular correlation structure (solid line) on to a single axis (ϕ^*) for the reaction $^{16}O(^{16}O,^{16}O^*[2_3^+, 11.52\ \text{MeV}] \rightarrow {}^{12}C_{g.s.}+\alpha)$ $^{16}O_{g.s.}$, compared with simulated angular correlation projections (dotted line) on to the same axis. The k and L values chosen for the simulation are shown on each plot. (a) The $E_{c.m.}=36$ MeV enhancement, (b) the $E_{c.m.}=37$ MeV enhancement.

TABLE I. Extension of Table 1 from Ref. [11] showing known elastic and inelastic channel resonances in the $^{16}O+^{16}O$ system, incorporating the new resonances measured in this work.

c.m. energy region (MeV)	Channel	Centroid (MeV)	Spin	Reference
24–27	Elastic	24.5	(16,18)	[28–32]
24–27	0_2^+	25.5	18	[9,10]
28–31	Elastic	29.5	(18–20)	[28–32]
28–31	0_2^+	29.3	(20,22)	[9,10]
28–31	3_1^-	28.1	20	[13]
28–31	3_1^-	30.0	(20,22)	[13]
28–31	4_1^+	30	(22,24)	This work
32–35	Elastic	35.0	(20–22)	[28–32]
32–35	0_2^+	33.6	(22,26)	[9,10]
32–35	3_1^-	35.0	(26,28)	[13]
36–39	0_2^+	38.2	24	[9]
36–39	Mutual 0_2^+	37.0	(20,22)	[11]
36–39	2_3^+	37	(22,24)	This work
36–39	4_1^+	36	(26,28)	This work
36–39	4_2^+	36	26	This work
36–39	4_2^+	39	26	This work

the spin deduced from our measurement, $J=26$ or 28.

The $E_{\text{c.m.}}\simeq 30$ MeV and 36 MeV enhancements observed in this work also overlap well in terms of energy with two similar structures reported by Balamuth *et al.* [9]. However, the spins assigned in this measurement, a single excitation to the 0_2^+, 6.05 MeV excited state in ^{16}O, were $J=18$ and $J=22$ for the $E_{\text{c.m.}}\simeq 30$ MeV and 36 MeV structures, respectively, and are not in agreement with the spins we have assigned at these center-of-mass energies.

The peak observed at $E_{\text{c.m.}}\simeq 30$ MeV is also partially correlated with a structure observed in the excitation function for single excitation to the 0_2^+, 6.05 MeV state at $E_{\text{c.m.}}\simeq 29.3$ MeV measured by Barrow *et al.* [10]. This structure was assigned a dominant partial wave of $L=20$ or 22 (assuming stretched coupling, $J=24$ or 26) and therefore overlaps reasonably well with our measured peak. The slight discrepancy between the energies of these structures may be associated with the broadness of the peak at 30 MeV in the present measurement. An enhancement has also been observed for elastic scattering in the $^{16}O+^{16}O$ system at $E_{\text{c.m.}}\simeq 29.5$ MeV by Maher *et al.* [27]. However, this was assigned a spin of $J=18$ or 20.

No spins were assigned to the bump observed in this work at $E_{\text{c.m.}}\simeq 39$ MeV because of the low statistics at this energy making comparisons with other enhancements difficult.

2. 4_2^+, 11.09 MeV excitation function

The enhancement observed in this excitation function at $E_{\text{c.m.}}\simeq 36$ MeV (assuming stretched coupling $J=26$) overlaps with a structure observed by Pate *et al.* [13] in the single excitation of ^{16}O to the 3_1^-, 6.13 MeV state (assigned spin was $J=26$ or 28).

An overlap in energy is also seen between the enhancement observed at $E_{\text{c.m.}}\simeq 36$ MeV and the enhancement observed by Balamuth *et al.* at $E_{\text{c.m.}}\simeq 36$ MeV [9] for the single excitation to the 0_2^+, 6.05 MeV excited state. However, the spin assigned by Balamuth *et al.* was J = 22 which does not agree with our assigned spin of $J=26$. A similar conclusion can also be drawn upon comparing the structures observed in this measurement and in the results reported by Balamuth *et al.* at $E_{\text{c.m.}}\simeq 39$ MeV where the spins were assigned values of $J=26$ and J = 24 respectively.

Additional overlaps in terms of energy between our enhancements at $E_{\text{c.m.}}\simeq 36$ MeV and $E_{\text{c.m.}}\simeq 39$ MeV and the work of Wells *et al.*, mutual excitation to the 3_1^-, 6.13 MeV [12], and Pate *et al.* [13], respectively, can be made. The authors, in both cases, were unable to assign spins to these enhancements making further comparison difficult.

B. Comparison of the 4_1^+, 10.35 MeV and 4_2^+, 11.09 MeV excitation functions

The peaks observed in the 4_1^+, 10.35 MeV and 4_2^+, 11.09 MeV excitation functions are at very similar center-of-mass energies. Of the three most notable peaks at $E_{\text{c.m.}}\simeq 30$, 36, and 39 MeV only the 36 MeV enhancement can be compared directly as it has been assigned a spin in both excitation functions whereas incomplete spin assignments for the other structures restrict comparison. The values for the $E_{\text{c.m.}}\simeq 36$ MeV enhancement agree well, $J=26$ or 28 for the 4_1^+, 10.35 MeV excitation function and $J=26$ for the 4_2^+, 11.09 MeV excitation function. The spins in both excitation functions agree more favorably with the work of Pate *et al.* [13] than that of Balamuth *et al.* [9].

The similarity between the excitation functions despite the strong structural difference between the two states suggests that strong coupling is occurring in the $^{16}O+^{16}O$ reaction or that the structure is dominated by resonances in the

entrance (elastic) channel. In this regard it should be noted that the relative population of these states may be important. The enhancement observed in the 4_2^+, 11.09 MeV excitation function has a much greater beam normalized yield, within the resolution of the measurement, suggesting that single excitation to this state is the dominant process and favored by the $^{16}O+^{16}O$ reaction.

C. The 2_2^+, 9.84 MeV and 2_3^+, 11.52 MeV excitation functions

Two possible peaks may be observed at $E_{c.m.} \simeq 32$ MeV and 36 MeV in the 2_2^+, 9.84 MeV excitation function. The structure at 36 MeV overlaps with the excitation function for single [13] and mutual [12] excitation to the 3_1^-, 6.13 MeV state in ^{16}O. However, due to the low statistics in this excitation function no firm spin assignments were possible.

The enhancement at $E_{c.m.} \simeq 37$ MeV in the 2_3^+, 11.52 MeV excitation function overlaps well with a structure observed in the excitation function for mutual excitation to the 0_2^+, 6.05 MeV excited state also at $E_{c.m.} \simeq 37$ MeV [11]. Furthermore, the spins determined by Wimer *et al.*, $J=20$ or 22, agree well with the spins determined in this measurement, $J=22$ or 24.

VI. SUMMARY

In conclusion, we have presented measurements, using the MEGHA strip detector array at the Australian National University (ANU), on the beam normalized yield for the reaction $^{16}O(^{16}O,^{16}O^* \rightarrow {}^{12}C_{g.s.}+\alpha)^{16}O_{g.s.}$, proceeding from excited states in ^{16}O above the particle decay threshold sampled over the center-of-mass energy range $E_{c.m.}=26-47$ MeV.

Various enhancements in the excitation functions for excitation to the 4_1^+, 10.35 MeV and 4_2^+, 11.09 MeV excited states have been reported and their energies and spins have been compared with previous work. The similarity of these excitation functions, despite the strong structural difference between the two states, suggests that strong coupling occurs in the $^{16}O+^{16}O$ system. Excitation functions for the excitation to the 2_2^+, 9.84 MeV and 2_3^+, 11.52 MeV levels in ^{16}O have also been presented.

In a previous publication Wimer *et al.* produced a useful table (Table 1 in Ref. [11]) summarizing the resonances in the $^{16}O+^{16}O$ system for which spins have been measured. To aid comparison, Table I in this paper is an extension of this, incorporating the new measurements from this work. It should be noted that any overlap between enhancements observed in this and previous work must be tentative due to the broadness of the structures seen and the broad energy step of the excitation function performed. This study has shown that the measurements can be carried out and that there is structured yield in the excitation functions. It is suggested that any future work on this system should utilize a finer energy step in measuring the excitation function.

ACKNOWLEDGMENTS

The authors wish to thank the staff of the Department of Nuclear Physics at the ANU for assistance in running the experiments. We acknowledge the financial support of the U.K. Engineering and Physical Sciences Research Council (EPSRC). The experimental work was performed under a formal agreement between the EPSRC and the ANU.

[1] K. A. Erb and D. A. Bromley, *Treatise on Heavy-Ion Science*, edited by D. A. Bromley, (Plenum, New York, 1984), Vol. 3, p. 201.
[2] N. Cindro, Riv. Nuovo Cimento **4**, 6 (1981).
[3] T. M. Cormier, Annu. Rev. Nucl. Part. Sci. **32**, 271 (1982).
[4] E. Almqvist, D. A. Bromley, and J. A. Kuehner, Phys. Rev. Lett. **4**, 515 (1960).
[5] T. M. Cormier *et al.*, Phys. Rev. Lett. **40**, 924 (1978).
[6] W. D. M. Rae, P. R. Keeling, and S. C. Allcock, Phys. Lett. B **184**, 133 (1987).
[7] M. Freer and A. C. Merchant, J. Phys. G **23**, 261 (1997).
[8] N. Cindro, Ann. Phys. (Paris) **13**, 289 (1988).
[9] D. P. Balamuth, T. Chapuran, C. M. Laymon, W. K. Wells, and D. P. Bybell, Phys. Rev. Lett. **55**, 2842 (1985).
[10] S. P. Barrow, R. W. Zurmühle, A. H. Wuosmaa, and S. F. Pate, Phys. Rev. C **46**, 1934 (1992).
[11] N. G. Wimer, S. P. Barrow, Y. Miao, C. Lee, J. T. Murgatroyd, X. D. Li, R. Antonov, and R. W. Zurmühle, Phys. Rev. C **56**, 1954 (1997).
[12] W. K. Wells, D. P. Bybell, and D. P. Balamuth, Phys. Rev. C **25**, 2512 (1982).
[13] S. F. Pate, R. W. Zurmühle, A. H. Wuosmaa, P. H. Kutt, M. L. Halbert, D. C. Hensley, and S. Saini, Phys. Rev. C **41**, R1344 (1990).
[14] B. Buck and J. A. Rubio, J. Phys. G **10**, L209 (1984).
[15] J. P. Elliott, J. A. Evans, and E. E. Maqueda, Nucl. Phys. **A437**, 208 (1985).
[16] R. A. Baldock, B. Buck, and J. A. Rubio, Nucl. Phys. **A426**, 222 (1984).
[17] P. Descouvemont, Phys. Rev. C **47**, 210 (1993).
[18] B. Buck, C. B. Dover, and J. P. Vary, Phys. Rev. C **11**, 1803 (1975).
[19] D. R. Tilley, H. R. Weller, and C. M. Cheves, Nucl. Phys. **A564**, 1 (1993).
[20] J. Zhang, D.Phil. thesis, University of Oxford, 1995.
[21] S. P. G. Chappell *et al.*, Phys. Rev. C **51**, 695 (1995).
[22] R. L. Cowin *et al.*, Nucl. Instrum. Methods Phys. Res. A **423**, 75 (1999).
[23] S. P. G. Chappell, W. D. M. Rae, and P. M. Simmons, Nucl. Instrum. Methods Phys. Res. A **396**, 383 (1997).
[24] M. Freer, Nucl. Instrum. Methods Phys. Res. A **383**, 463 (1996).
[25] S. P. G. Chappell and W. D. M. Rae, Phys. Rev. C **53**, 2879 (1996).

[26] S. P. G. Chappell, W. D. M. Rae, C. A. Bremner, G. K. Dillon, D. L. Watson, B. J. Greenhalgh, R. L. Cowin, M. Freer, and S. M. Singer, Phys. Lett. B **444**, 260 (1998).
[27] J. V. Maher, M. W. Sachs, R. H. Siemssen, A. Weidinger, and D. A. Bromley, Phys. Rev. **188**, 1665 (1969).
[28] O. Tanimura and T. Tazawa, Nucl. Phys. **A346**, 266 (1980).
[29] A. Gobbi, R. Wieland, L. Chua, D. Shapira, and D. A. Bromley, Phys. Rev. C **7**, 30 (1973).
[30] A. Tohaski, F. Tanabe, and R. Tamagaki, Prog. Theor. Phys. **45**, 980 (1971).
[31] N. Rowley, J. Phys. G **6**, 697 (1980).
[32] W. R. Gibbs, Phys. Lett. **103B**, 281 (1981).